PAPER

Porphyrin molecules boost the sensitivity of epitaxial graphene for NH_3 detection

IOP Publishing Journal of Physics: Condensed Matter
J. Phys.: Condens. Matter **29** (2017) 065001 (11pp) doi:10.1088/1361-648X/29/6/065001

Porphyrin molecules boost the sensitivity of epitaxial graphene for NH_3 detection

I Iezhokin[1], D den Boer[1,3], P Offermans[2], M Ridene[1], J A A W Elemans[3], G P Adriaans[1] and C F J Flipse[1]

[1] Molecular Materials and Nanosystems, Eindhoven University of Technology, 5600 MB Eindhoven, The Netherlands
[2] Holst Centre/IMEC-NL, 5605 KN Eindhoven, The Netherlands
[3] Radboud University, Institute for Molecules and Materials, Heyendaalseweg 135, 6525 AJ Nijmegen, The Netherlands

E-mail: c.f.j.flipse@tue.nl

Received 12 July 2016, revised 26 October 2016
Accepted for publication 1 November 2016
Published 19 December 2016

Abstract

The sensitivity of quasi-free standing epitaxial graphene for NH_3 detection is strongly enhanced by chemical functionalization with cobalt porphyrins resulting in a detection limit well below 100 ppb. Hybridization between NH_3 and cobalt porphyrins induces a charge transfer to graphene and results in a shift of the graphene Fermi-level as detected by Hall measurements and theoretically explained by electronic structure calculations.

Keywords: sensing, quasi-free standing epitaxial graphene, NH_3 adsorption, cobalt porphyrin functionalization, electronic structure calculations

(Some figures may appear in colour only in the online journal)

Introduction

The electronic properties of graphene are highly sensitive to the interaction of molecules at its surface. The binding of molecules alters the carrier density and the charge transfer [1–5], which results in changes of the conductance of the graphene sheet. Even a low number of molecules at the surface can already lead to a measurable effect [1] and therefore graphene is a promising material to be used as a chemical sensor. The sensitivity and selectivity for gas sensing of graphene devices is determined by the chemical interaction between the molecule and the graphene surface, i.e. the electronic structure of both. Exploiting the full potential offered by graphene in sensing applications requires extensive fundamental studies on the behavior of the surface of graphene upon their chemical, electronic interaction with gas and receptor molecules. Surface non-covalent modification with receptor molecules can allow for an enhanced sensing performance in terms of selectivity and sensitivity.

The functionalized graphene sensors used in this work are based on quasi-free standing epitaxial grapheme [6, 7]. A major advantage of epitaxial graphene over the other graphene allotropes is its clean fabrication method which avoids processing pollutants such as poly(methylmethacrylate) (PMMA) [2] that can influence the sensing. Moreover, it allows for easy up-scaling of device fabrication. Recently, we have shown highly sensitive epitaxial graphene gas sensors for NO_2 with a sub-ppb sensitivity. These sensors, however, are not sensitive to for instance NH_3 and CO [8].

Metalloporphyrins (MP) are aromatic square plane molecules with incorporated metal atoms in a tetradentate fashion (Cu, Fe, Co etc).These molecules are an attractive platform for gas sensing because they are able to specifically bind certain analytes [9, 10] as axial ligands to their metal centers. Particularly cobalt porphyrins are known to bind to amines [11, 12]. In the case of MPs and NH_3, this interaction is associated with the nature of the central metal ion of the MPs. In comparison to other transition metal ions, the formation of the complex between a cobalt porphyrin and a NH_3 ligand is most favorable among other metal-ligand pairs due to its large charge transfer [13].

The sensing properties of transition metal cobalt porphyrins are nicely demonstrated in [15], for the case of a porphyrin thin-film FET as a gas sensor; however, the very low electrical conductivity of the porphyrin is a significant drawback for chemi-resistive sensors [16]. Indeed, there are many other

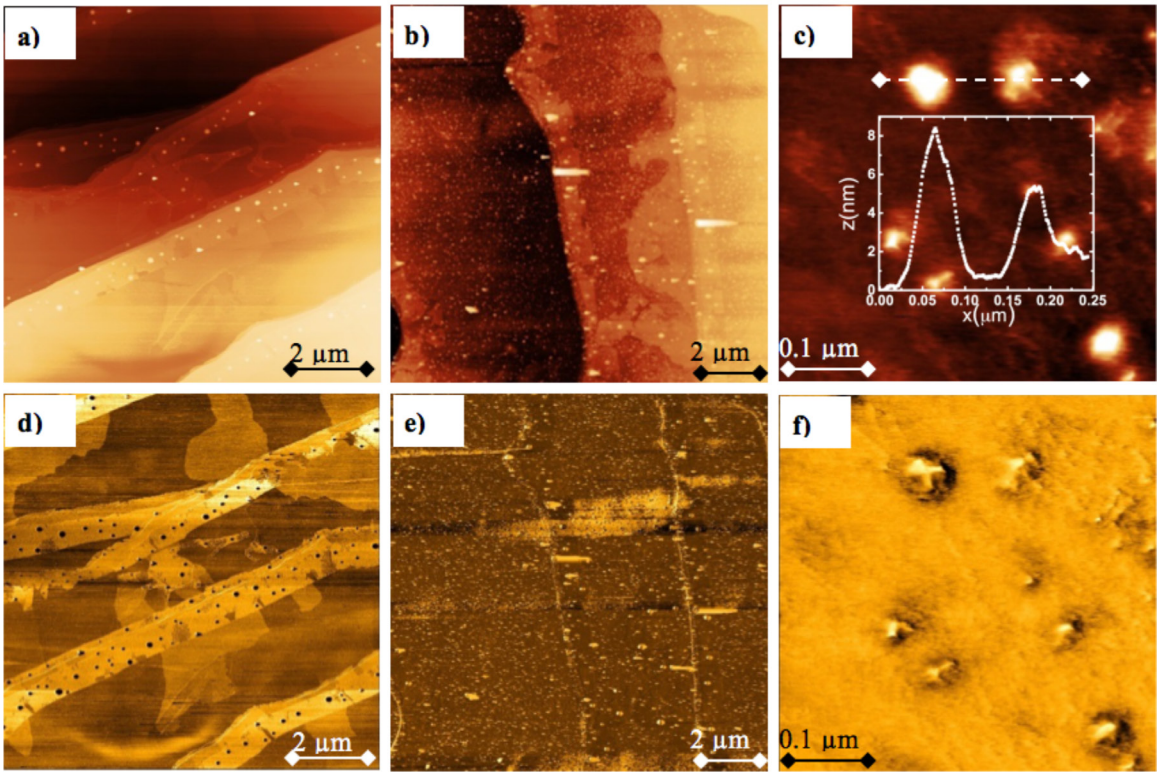

Figure 1. Atomic force micrograph of QFeG and functionalized with CoMP porphyrin. Height image (a) showing terraces together with AFM phase image (d) for clean QFeG sample. Height (b) and phase (e) AFM images for CoMP-QFeG sample. Zoomed height (c) and phase (f) images show the morphology of CoMP-QFeG surface. The inset at (c) shows a cross-section of the typical clusters on the surface of functionalized graphene sample.

examples of devices based on the trans-conductance approach which could overcome the problem of the low porphyrin conductivity, using different types of porphyrins for surface functionalization [17, 18]. One of the promising examples of such an approach has been shown for InAs nanowires functionalized with a metalloporphyrin (Hemin) demonstrating a ppb-level sensitivity to NO_x gas family species [19].

The morphology of the porphyrin molecules on surfaces is an important issue to use them for the chemical modification of the graphene surface; it is known that they can form self-assembled monolayers on graphite after stabilizing them with alkyl chains [20].The deposition of metal-porphyrins on graphene leads to a non-covalent functionalization, i.e. their aromatic core is non-covalently bonded to the graphene surface through the π-system, while the enhanced π–π electron interaction will influence the electronic structure of graphene and lead to a charge transfer and/or a shift of the Fermi level [21, 22].

In the current paper, we functionalize quasi-freestanding graphene by cobalt porphyrin deposition to improve the sensitivity for detecting NH_3 molecules. Furthermore, we will address the chemical functionalization role of a cobalt porphyrin molecule layer as an important intermediate layer between the graphene surface and the adsorbing molecule NH_3. Pristine epitaxial and exfoliated graphene are not sensitive enough for the detection of NH_3 in ppb range due to a poor chemical interaction [23, 24]. However, NH_3 in chemical contact with a Co-porphyrin layer alters the carrier density in graphene, resulting in a ppb (parts per billion) range NH_3 sensitivity as determined by Van der Pauw resistance and *in situ* Hall measurements. These methods provide advantages for real time monitoring of the graphene sheet resistance upon NH_3 adsorption.

Results and discussion

We used quasi-freestanding epitaxial graphene (QFeG) samples [8] for NH_3 sensing experiments. The QFeG samples were grown by thermal decomposition on the siliconcarbide (0001) surface and show a linear electron dispersion at the K-point. The Co-porphyrin layer(s) were formed by physisorbing 5,10,15,20-*meso*-tetrakis-nonadecylporphyrinato cobalt(II) (CoMP) molecules on the graphene surface by dropcasting, followed by drying, as shown in figure 2, in a nitrogen flow. The morphology was obtained with an Atomic Force Microscope (AFM) as is shown in figure 1.

The topology and phase image of clean QFeG are presented in figures 1(a) and (d) respectively. The terraces are typically 4 μm in width and have a step-height of about 10 nm; in the phase image (figure 1(d)), recorded simultaneously with the topology, the terraces consist mainly of single layer (dark) graphene with a narrow region of bilayer (bright) graphene at the terrace edges. The topology of CoMP-QFeG is shown in figure 1(b) and the corresponding phase image in figure 1(e). In the phase image the contrast between single

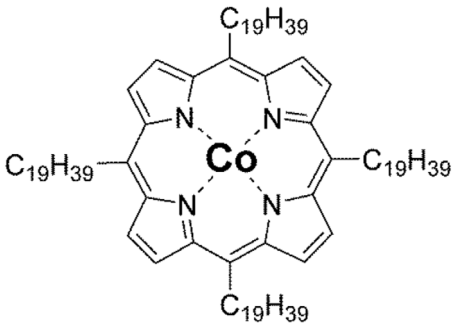

Figure 2. Structure of the CoMP molecule.

and bilayer is not observed and the terraces look very homogeneous which can be understood due to the presence of CoMP molecules as a closed layer or layers on the graphene surface. A zoomed-in height and phase image, figures 1(c) and (f) respectively, of the CoMP-QFeG surface shows additionally clusters with a 50 nm diameter and a height around 10 nm (see inset figure 1(c)). These clusters cover about 5% of the CoMP layer surface and are likely formed by aggregated CoMP molecules. In the sensing experiments, the device current passes mainly through the graphene layer and not through the porphyrin layer, as it has already been shown in literature that the conductance of the porphyrin layer is much lower; the carrier mobility of the porphyrin layer is 5×10^{-4} cm^2 V^{-1} s^{-1} [17] compared to 1200 cm^2 V^{-1} s^{-1} for clean QFeG before functionalization and was measured with van der Pauw method.

Chemical characterization is performed by x-ray photoelectron spectroscopy (XPS) as is shown in figure 3. The adsorption of the porphyrin molecules on the graphene layer grown on SiC has been investigated by means of core-level photoemission. In the XPS wide scans for clean QFeG and CoMP-QFeG in figures 3(a) and (b) a contribution of carbon, silicon as well (figure A4(c) and (d) respectively) as nitrogen and cobalt after porphyrin dosing is present. In the porphyrin covered sample also a relative large contribution of oxygen is visible, which can be explained by H_2O adhered to the porphyrin molecules during the adsorption process on grapheme [25].

In figure 3(a) the C-1*s* for QFeG contribution at 284.3 eV eV can be assigned to the graphene contribution (C atoms in sp^2 configuration). The component located at 282.6 eV is attributed to the substrate bulk-SiC. This peak is shifted to lower binding energies in comparison to epitaxial graphene due to the pyroelectric effects in bulk SiC, resulting from a strong polarization effect [26].

Separately we have measured XPS spectra for CoMP molecules deposited on a glass substrate, using a flood gun to prevent charging due to the insulation glass substrate, see figure 3(c). This spectrum was fitted with three pseudo-Voight-profiled components: a peak centered at 285.9 eV and at 284 eV attributed to the porhyrin ring [27–30], a contribution situated at 284.6 eV ascribed to the carbons, directly connected to the N-atoms; at 288.2 eV a shake-up contribution associated with the pyrrole carbons is visible [28].

After functionalization of QFeG with cobalt porphyrins there is almost no shift of the sp^2 contribution and a shift

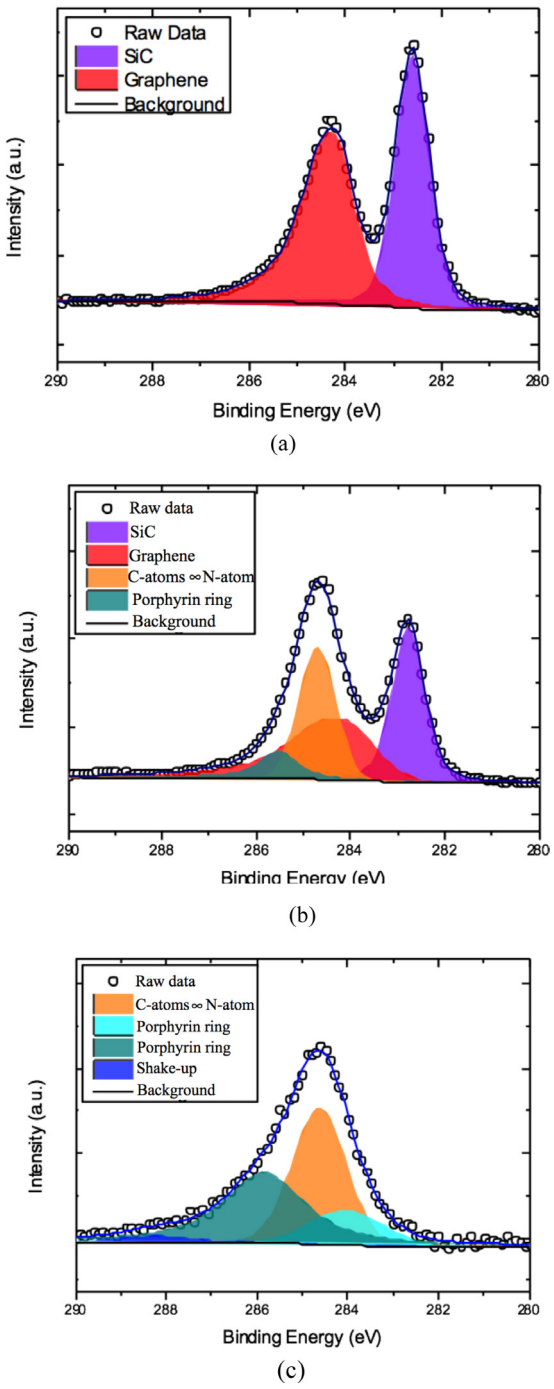

Figure 3. XPS data of the C 1*s* core-level of (a) QFeG sample, (b) CoMP functionalized QFeG. (c) CoMP on glass.

of 0.2 eV to higher binding energies for the C-contribution of SiC; this latter shift is probably due to a reduced SiC screening capability of the graphene C-sp^2 states caused by the strong hybridization with the localized Co-3*d* states close to the Fermi-level as is shown in bandstructure calculations in figure 6(b) which will be discussed later.

The N-1*s* peak is not very sensitive to the thickness of the CoMP layer without alkyl chains as is shown by Hermanns [31] and Bai [32]; they obtained 398.5 eV for the N-1*s* of the CoMP for thicknesses between 1 and 10 ml. Our value 399.2 eV, see figure A4(b), is 0.7 eV higher compared to Bai

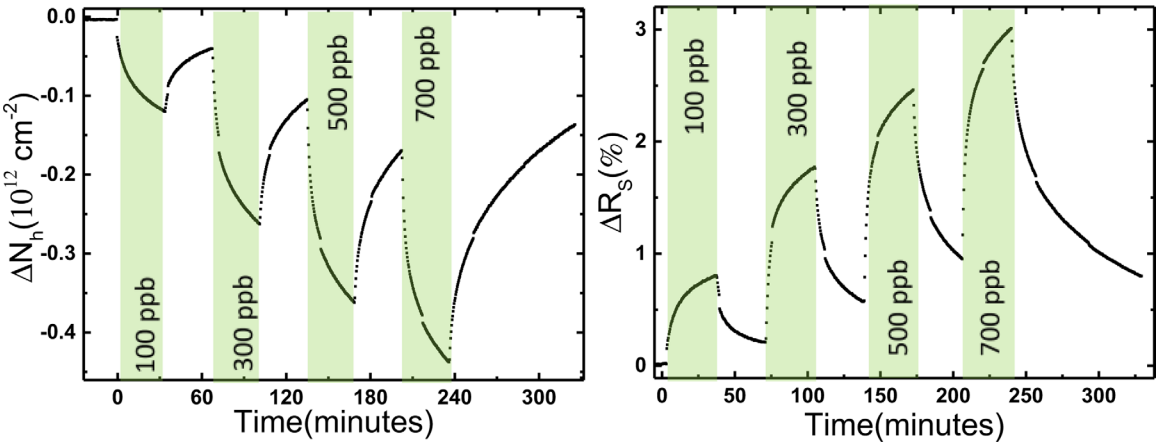

Figure 4. Carrier concentration (a) and relative resistance changes (b) of CoMP-QFeG sensor exposed first to pure N_2 and then to a sequence of 100 ppb ($t = 0$ min), 300 ppb ($t \sim 65$ min), 500 ppb ($t \sim 120$ min), 700 ppb ($t \sim 210$ min) of NH_3 gas.

et al for CoMP without alkyl chains on on Au (1 1 1), possibly as a result of the larger metallic screening of gold compare to graphene. The Co-2*p* peak shifts from 780 eV (1 ml) to 781.6 eV for 10 ml [17]. Our Co-2*p* contribution is 780.9 eV, 0.9 eV higher than the value of Bai *et al* [32]. This could as is shown in figure A4(a) indicate that we have more than 1 ml of CoMP and/or a layer of CoMP with a large chemical shift due to a reduced charge screening effect of graphene compared to metallic Au(1 1 1), similar as the chemical shift of N-1*s*.

Hall experiments reveal charge doping effects due to gas adsorption on the graphene surface, determining the type and the amount of charge carriers in the graphene by the energy difference between the Fermi level and the Dirac point as is shown in equation (1). This simple expression is based on the linear dispersion of the density of states near the Dirac point, which is valid up to 1 eV [33] for QFeG; the charge carrier concentration is then given by:

$$N_e(N_h) = \frac{1}{\pi(\hbar\vartheta_F)^2}(|E_F - E_D|)^2, \qquad (1)$$

where N_e (N_h) is the electron (hole) density, ϑ_F the Fermi velocity, E_F is the Fermi level position and E_D is the energy position of the Dirac point. The initial and final doping level of the sample before and after the porphyrin functionalization procedure was determined by obtaining measurements of the major carrier concentration (*n* or *p*) mobility and the sheet resistance R_S. Prior to the measurements, the CoMP functionalized QFeG sensors were stabilized, i.e. the resistance signal is stable within a few percent under a 3 slm flow of pure N_2 after 1 h before the NH_3 gas was added to the N_2 flow. Figures 4(a) and (b) show the functionalized QFeG sensor response due to NH_3 adsorption. The response is given by the relative change in resistance $(R_S - R_{S0})/R_{S0}$ (%), where R_{S0} is the sheet resistance prior to exposure and induced carrier concentration is given by $N_{e(h)}$–$N_{e(h)0}$, where $N_{e(h)0}$ are the sheet carrier concentration prior to exposure of NH_3.

The relative response and induced charge carrier concentration of both samples were measured using a sequence of 30 min NH_3 exposure with concentrations of 100 ppb, 300 ppb, 500 ppb and 700 ppb respectively. Between each exposure the gas supply is stopped for 30 min, allowing the sample to recover under a pure N_2 flow. The CoMP-QFeG sample shows an increase in the response (figure 4(b)) upon NH_3 exposure, which after 30 min results in a steady-state response of 0.5%, suggesting an equilibrium between the gas absorption and desorption. During the same time, the induced carrier concentration decreases to a value of 1.5×10^{11} cm^{-2}. In the absence of NH_3, the sensor recovers from gas exposure by the desorption of NH_3, which is governed by a reduction of the response. Each subsequent exposure at increasingly higher NH_3 concentration corresponds to an increased sensor response. The CoMP-QFeG sensor does not recover completely within the allowed recovery time. However, full recovery is possible without annealing given a sufficient recovery time as is shown in figure A6 of the appendix. The recovery time can be speeded up by annealing under the N_2 flow.

Figure 5 shows the performance difference in NH_3 sensitivity for clean QFeG and CoMP-QFeG. Clean QFeG samples show a negligible sensitivity to NH_3 gas as was theoretically predicted by Wehling *et al* [24] and as has been shown experimentally by Iezhokin *et al* [8], also confirmed in figure A1. In contrast, the Co-MP functionalized QFeG gives a clearly observable sensitivity which can be explained by electronic structure calculations.

In order to understand the doping effect of the graphene layer in the presence of a Co-porphyrin layer, we conducted spin polarized calculations within the LSDA as implemented in the SIESTA computational code [34]. A (7×7) graphene unit cell containing 98 carbon atoms was used. Sampling of the brillouin zone takes place by a ($5 \times 5 \times 1$) shifted Monkhorst–Pack grid [35], while a mesh cutoff energy of 300 Ry has been imposed for real-space integration. The structure has been relaxed until forces were less than 0.05 eV Å^{-1}.

The bandstructure for the porphyrin molecule positioned on graphene after relaxing the structure is indicated in figure 6, which is in agreement with STM experiments of CoMP on graphite (HOPG) [36] where their aromatic planes cofacially are arranged within the graphene plane. The alkyl groups are not taken into account in the calculation because they only facilitate self-assembly of the porphyrin-alkyl groups and the physisorption on graphene. It reveals the characteristic linear

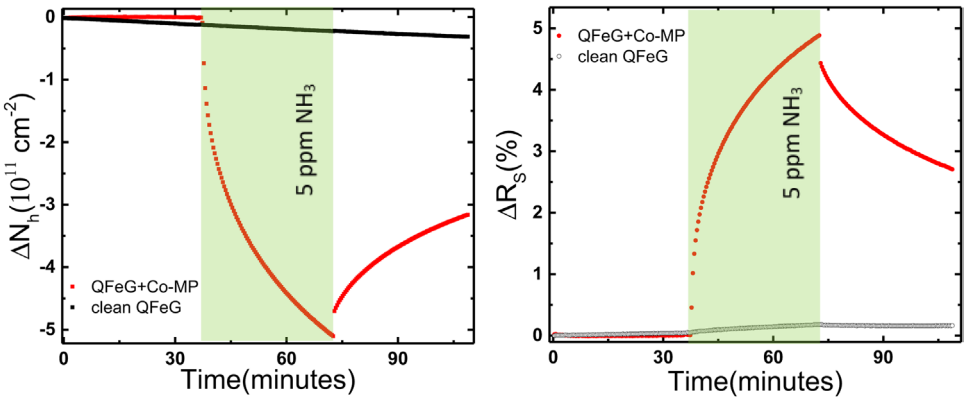

Figure 5. Sensitivity clean and functionalized CoMP quasi-free standing graphene sensor to NH_3 exposure. Carrier concentration (a) and relative resistance (b) change of CoMP functionalized QFeG during exposure to 5 ppm NH_3 gas.

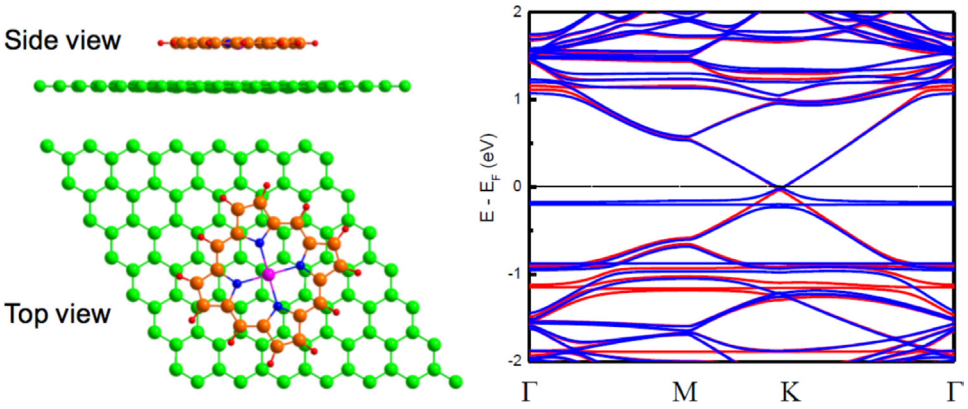

Figure 6. (a) Surface structure and (b) spin-polarized bandstructure of graphene with one Co-porhyrin molecule adsorbed; blue = spin-down and red = spin-up.

dispersion close to the K-point of graphene, changed by the hybridization with the filled Co-MP 3*d*-states at 0.2 eV below E_F and a contribution at ±1 eV. The Co-3*d* spin-states seems to be opposite to the expected spin direction; the Co-3*d* state at 0.2 eV below E_F is a spin-down state due to the hybridization with the N-states, which carries a spin-up magnetization and the Co-3*d* at 1 eV below E_F is a spin-up state for the same reason. The hybridization of these spin-polarized states (red = spin-up, blue = spin-down) does not change the Fermi-energy position in respect to the Dirac point, indicating that there is no obvious *n*-or *p* doping effect due to the Co-porphyrin adsorption on graphene. This is in contrast to the *p*-doping effect as is obtained from the transport experiments in figure 4. The most probable reason for the absence of a Fermi-level shift is a charge transfer process due to a *hybridization* between the graphene layer and the porphyrin molecule. Chilukuri *et al* [14] showed for CoMP without alkyl chains adsorption on graphite (HOPG), using the van der Waals-DF LDA functional in VASP, that 0.6 electrons are redistributed from the graphite substrate to the Co-MP molecule. A hybridization between the Co-3d_z [2] and the C-p_z states takes place near the Fermi-level after cobalt porphyrin functionalization. Due to the so called 'push back' effect [37] caused by Pauli repulsion, which is not taken into account in our electronic structure calculations, charge localization occurs mostly towards the porphyrin, thereby forming an interface dipole. This effect explains the work-function reduction due to an interface dipole formation as was measured for graphite [34]. We expect that this phenomenon of electron donation from graphite will also occur for graphene due to a similar sp^2 electron configuration.

The calculated electronic structure results for NH_3 adsorbed on the Co atom of the porphyrin molecule on graphene in figure 7 clearly shows a *n*-doping of the graphene layer due to the *N* spin-up states of NH_3 which are hybridized with the Co-3*d* spin-down states, forming a very localized spin-polarized state at the Fermi-level. As a results the Fermi-level shifts ~0.2 eV, similar to the value determined from the experimentally found carrier concentration *N* of figure 5 and applying equation (1). The charge redistribution after the NH_3 adsorption causes now a rigid shift of the Fermi-level in the bandstructure calculation, similar as the simple model from equation (1) predicts. In figure 8 the density of states projected on the N- and H-atoms of NH_3 clearly shows the main difference in the HOMO level position of NH_3 for functionalized and non-functionalized graphene. The very localized HOMO level state, hybridized with the Co-3*d* spin-down states, at the Fermi-level in functionalized graphene pushes the Fermi-level position up with respect to the Dirac point, due to the strong hybridization also with the graphene states near the Fermi-level, thereby explaining the *n*-doping of graphene.

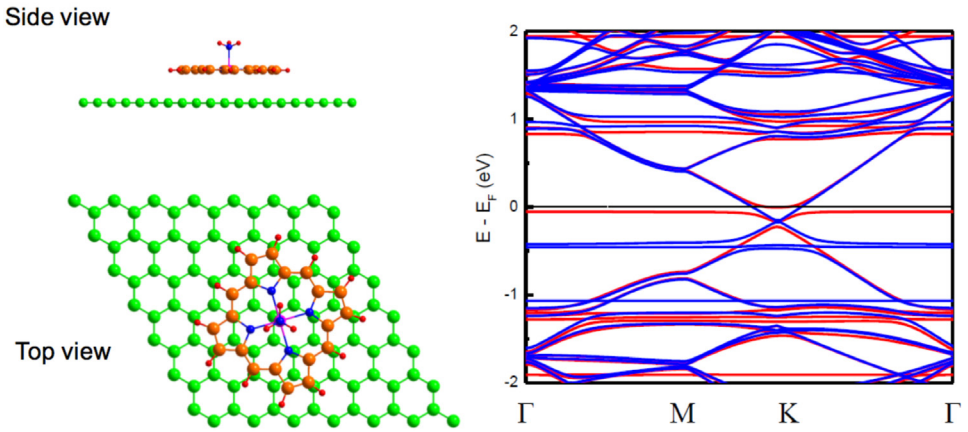

Figure 7. (a) Surface structure and (b) spin-polarized bandstructure of graphene with one Co-porhyrin and one NH_3 molecule adsorbed; blue = spin-down and red = spin-up.

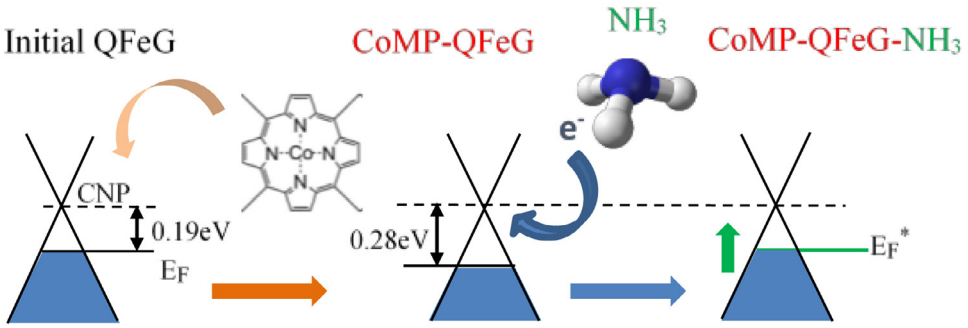

Figure 8. Projected density of states (PDOS) on nitrogen and hydrogen atoms. (a) For a single NH_3 molecule adsorbed on QFeG. (b) For a NH_3 molecule adsorbed on Co-porphyrin functionalized QFeG.

As we indicated in the morphology part, it is not clear from the AFM images if one or more Co-MP layers are deposited on graphene. Important is if the thickness plays an important role for the NH_3 adsorption and what the possible effects on the electronic structure might be. The electronic structure for a two-layer stack of Co-MP molecules adsorbed on graphene is calculated and the results are shown in appendix figure A2. The stacking of the Co-MP layers relaxes as is shown in appendix figure A2(a) with the two Co-atoms on top of each other, even if there is an initial lateral distance of 2 Å before relaxing the structure between the two porphyrin layers. A stacking of two porphyrin layers gives rise to a 0.2 eV upward shift of the Fermi-level, *n*-doping the graphene layer. The experimental Hall experiments show the opposite effect, a hole doping shift of 0.2 eV, indicating that it is not very likely that the graphene surface contains more than a single porphyrin layer. Also the adsorption of a NH_3 molecule on a two-layer stack of porphyrin molecules is not thermodynamically stable as obtained from our electronic structure calculations, which indicates that a two or more layer stack of porphyrins is not expected to be present on graphene in our experiments.

The increased sensitivity of CoMP-QFeG for NH_3 is shown in figures 4 and 5 and can be explained by a relatively simple model [8] which takes into account the position of the Fermi-energy: for QFeG, the electron doping present in epitaxial graphene is cancelled by hydrogen intercalation ($N_{h0} = 2.6 \times 10^{12}$ cm^{-2}; $E_F - E_D = 0.19$ eV; $\mu_{QFeG} = 1200\,\text{cm}^2\,\text{V}^{-1}\,\text{s}^{-1}$; $R_S = 1970\ \Omega$), repositioning the Fermi-level closer to the Dirac point. As the density of states in graphene is linearly proportional to the energy (equation(1)), the sheet resistance, being inversely proportional to N, shows the largest variation with N when the Fermi level aligns with the Dirac point. Thus, in the case of the CoMP adsorption, the sp^2 state dispersion at the K-point is slightly modified by the hybridization with the localized Co-3*d* states; however, this disturbance of the linear dispersion occurs below 0.2 eV binding energy below E_F, whereas for NH_3 adsorption on CoMP, the very localized NH_3 HOMO/Co-3*d* spin state *at the Fermi-level* strongly changes the charge distribution, causing the large change in the sheet resistance.

Finally, figure 9 shows a sensing evolution model for CoMP and subsequent NH_3 adsorption on QFeG. After the deposition of the Co-porphyrins, the Dirac point of functionalized CoMP-QFeG is almost 0.3 eV above the Fermi level (and hence the graphene is *p*-doped). Additional NH_3 adsorption causes electron doping in QFeG as was discussed in the previous paragraphs. This results in an upwards shift of the Fermi-level and improves the sensitivity.

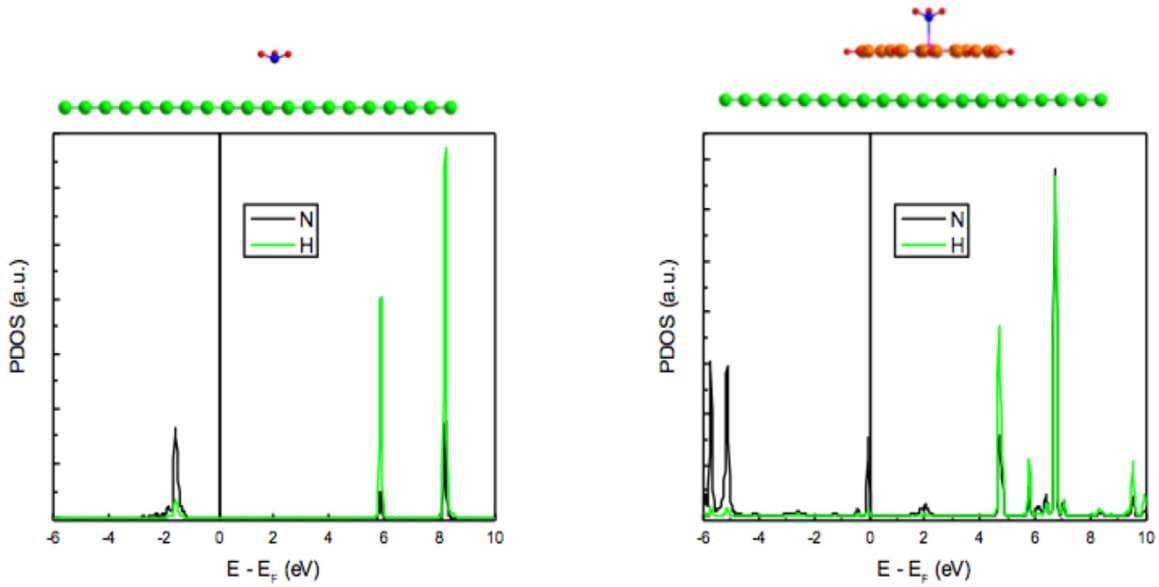

Figure 9. Schematic illustration of the sensing procedure for NH_3 adsorption on QFeG and the corresponding resistance and carrier concentration effects.

Conclusions

We have measured the response of cobalt porphyrin functionalized quasi free standing epitaxial graphene to NH_3 by means of electrical response measurements. QFeG shows a negligible response to NH_3 [8]. After functionalization the sensitivity of the QFEG to NH_3 is strongly enhanced resulting in a limit of detection well below 100 ppb NH_3 comparable to functionalized graphene systems, e.g. a 5% resistance increase is shown for 8 ppm NH_3 exposure by Zanjani *et al* [38].

Electronic structure calculations explain the *n*-doping effect of quasi free standing graphene after NH_3 chemisorption on the cobalt site of the porphyrin molecule by a small shift of the NH_3 HOMO level towards the Fermi-level and thereby boosting the electron transfer from graphene to the CoMP molecule.

Acknowledgments

We would like to thank C van Helvoirt for support during XPS measurements. J A A W E acknowledges the European Research Council (ERC Starting grant NANOCAT—259064) and the Netherlands Ministry of Education, Culture and Science (Gravity program 024.001.035). M R and I I acknowledge financial support by the Dutch Organization for Scientific Research (NWO) under Project No. 11447 and FOM.

Appendix

A.1. Methods

A.1.1. Sensor fabrication. Quasi-freestanding epitaxial graphene (QFeG) samples are used as substrate material for gas sensing [8]. QFeG samples are grown by thermal decomposition on the silicon (0 0 0 1) side of a $4 \times 4\,mm^2$ insulating 6H-SiC wafer piece from II to VI Inc. For the growth of eG we followed the procedure described by Emtsev *et al* [6]. The result is a decoupled layer of graphene supported by a buffer layer, which consists of a carbon layer strongly bonded to the substrate. For the QFeG samples we used a similar procedure as developed by Riedl *et al* [7].The result is a graphene layer which is decoupled from the hydrogen passivated SiC substrate. Subsequently, metal Au (50 nm)/Cr(2 nm) contacts were evaporated for all samples through metal mask and the sensors were wire bonded to a substrate with extended contacts to perform Hall measurements.

A.2. Synthesis of CoMP

Step 1: To 1 liter of dichloromethane, 1.01 g of freshly distilled pyrrole (15.0 mmol), 4.44 g of eicosanal (15.0 mmol) and 1 ml of trifluoroacetic acid (13.1 mmol) were added and the solution was stirred for 1.5 h at room temperature under an argon atmosphere. To the stirring solution 2.50 g of 2,3-dichloro-5,6-dicyano-1,4-benzoquinone (11.0 mmol) was added and the mixture was stirred for 1 h under argon at room temperature. To the stirring solution, 1.5 ml of triethylamine (10.8 mmol) was added and the solution was stirred for 30 min. The solvent was evaporated and the product was purified by silica column chromatography with chloroform as eluent to yield 12% of 5,10,15,20-*meso*-tetrakis-nonadecylporphyrin (0.45 mmol) as a brown solid. MALDI-TOF MS: *m/z* calculated for $C_{96}H_{166}N_4$: 1375.35; found: 1376.2 $(M + H)^+$. ^{1}H-NMR ($CDCl_3$, 500 MHz): $\delta = 9.47$ (s, 8H, H1), 4.93 (t, 8H, $^3J_{HH} = 7.8$ Hz, H2), 2.52 (qu, 8H, $^3J_{HH} = 7.8$ Hz, H3), 1.80 (qu, 8H, $^3J_{HH} = 7.8$ Hz, H4), 1.25 (br, 120H, H5), 0.87 (*t*, 9H, $^3J_{HH} = 6.8$ Hz, H6), −2.63 (*s*, 2H, H7). ^{13}C NMR ($CDCl_3$, 125 MHz): $\delta = 118.4$ (*meso*-C), 38.8 ($4 \times CH_2$), 35.6 ($4 \times CH_2$), 31.9 ($4 \times CH_2$), 30.7 ($4 \times CH_2$), 29.7 ($4 \times CH_2$), 29.4 ($4 \times CH_2$), 22.7 ($4 \times CH_2$), 14.1 ($4 \times CH_3$). Elemental Analysis calculated for $C_{96}H_{166}N_4$: C 83.77, H 12.16, N 4.07. Found: C 83.81, H 12.03, N 4.16.

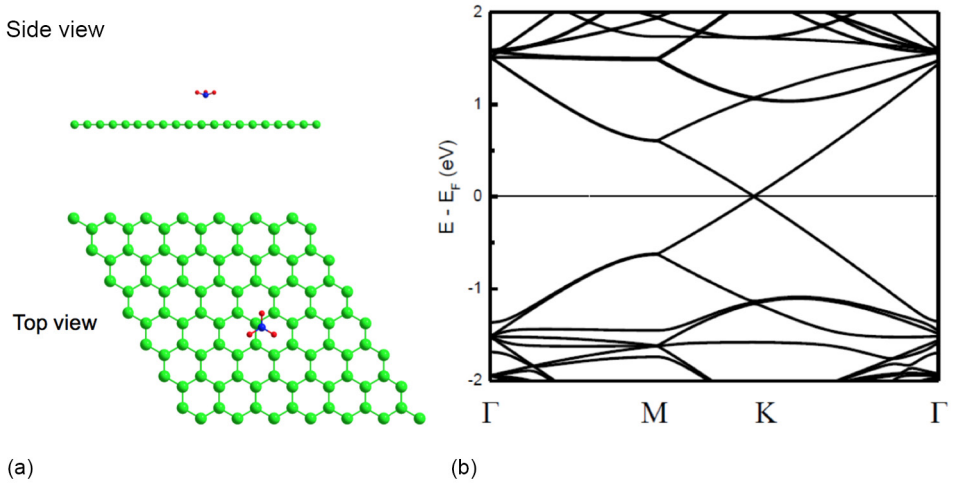

Figure A1. (a) Surface structure and (b) bandstructure of graphene for a single NH_3 adsorbed on grapheme.

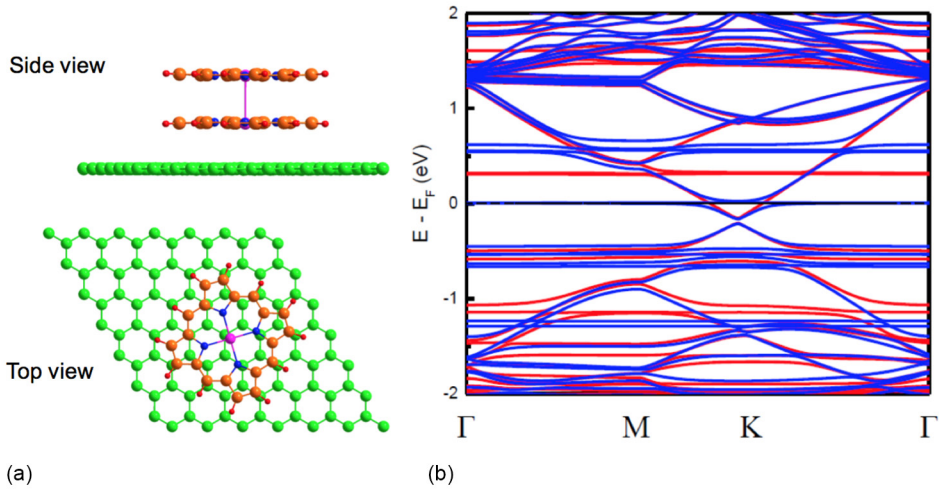

Figure A2. (a) Surface structure and (b) bandstructure of graphene with a 2 Co-porphyrin molecule stack.

Step 2: To a stirring solution of 0.30 g 5,10,15,20-*meso*-tetrakis-nonadecylporphyrin (0.22 mmol) in a 50 ml 4:1 chloroform:methanol (v/v) mixture, 0.44 g cobalt(II) acetate tetrahydrate (1.77 mmol) was added under an argon atmosphere. After refluxing for 16 h, the solvent was evaporated and the product was purified by a (neutral) alumina column with chloroform as eluent to yield 98% of darkred 5,10,15,20-*meso*-tetrakis-nonadecylporphyrinato cobalt(II) (CoMP). MALDI-TOF MS: *m/z* calculated for $C_{96}H_{164}CoN_4$: 1432.23; found: 1431.5. UV–vis ($CHCl_3$): λ_{max} 412, 540 nm. Elemental Analysis calculated for $C_{96}H_{164}CoN_4$: C 80.45, H 11.53, N 3.91. Found: C 81.20, H 12.22, N 3.38.

A.3. Co-porphyrin layer formation

Prior to functionalization with Co-porphyrins, the sample was annealed under N_2 gas flow at a temperature of 150 °C using the resistive heater implemented into the sample kit of the machine for 30 min. To avoid atmospheric doping after the annealing step, the graphene sample was immediately transferred to a *n*-heptane solution. The MP—layers were formed in two steps, first the graphene was cleaned by immersing the graphene sample for 8 h in a *n*-heptane solution and subsequently a 8×10^{-6} M CoMP solution in *n*-heptane was drop-casted on top of the substrate, followed by drying in a nitrogen

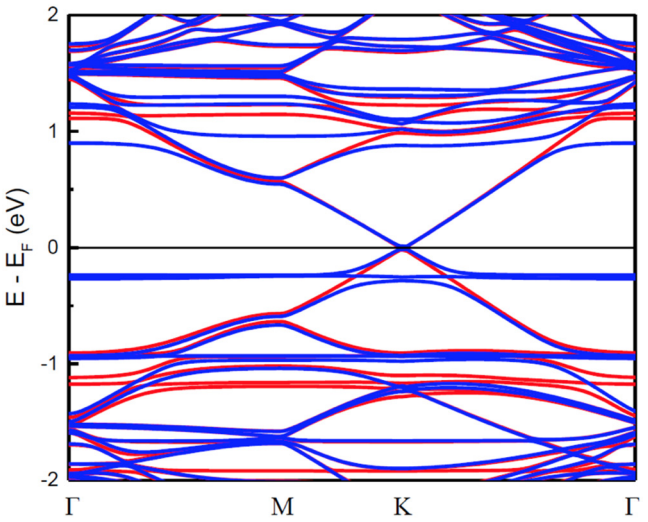

Figure A3. bandstructure of graphene with a Co-porphyin molecule co-adsorbed with a H_2O.

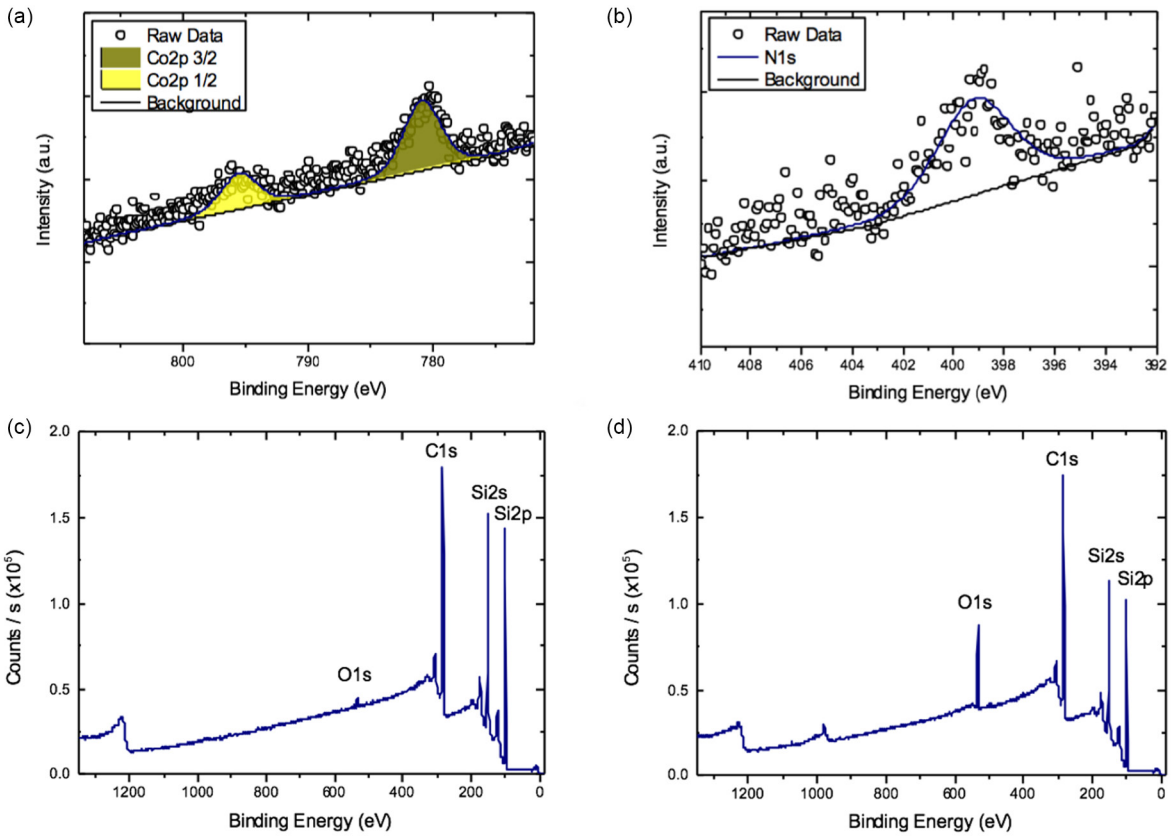

Figure A4. (a) XPS Co 2*p* core-level of CoMP functionalized QFeG. (b) XPS N-1*s* core level of CoMP functionalized QFeG. (c) XPS wide energy scan of QFeG. (d) XPS wide energy of CoMP functionalized QFeG.

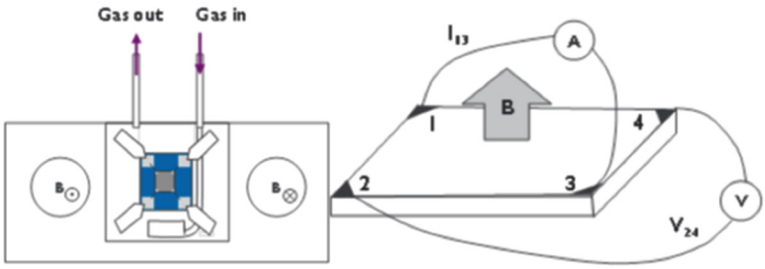

Figure A5. (a) Sketch of the used setup. A Van-der-Pauw configuration is used to measure sample resistance and Hall voltage. The graphene sample is wire bonded to a non-magnetic substrate providing large contact pads with For the measurement of the Hall voltage, the orientation of the magnetic field is changed by the use of two movable permanent magnets with opposite polarization. (b) Sketch of a 4-point Hall voltage measurement in the Van-der-Pauw configuration. The Hall voltage is derived using $V_{-\mathrm{H}} = (V13 + V24 + V31 + V42)/8$, with $Vij = Vij,P - Vij,N$, where P and N denote the different polarizations of the magnetic field.

flow. Layers were characterized by AFM technique. These measurements were performed with a Veeco Multi-Mode NanoScope, enclosed in a chamber with multiple layers of sound-damping materials for acoustic isolation. The measurements were done in tapping mode using silicon tips purchased by Nanosensors (type PPP-NCHR-20).

X-ray photoelectron spectra (XPS) where performed by K-Alpha XPS system (Thermo scientific) with flood source for charge compensation. This allows for the study of polymers without the need to make any adjustment to the charge compensation conditions. XPS uses Al K-alpha photons which have an energy of 1486.7 eV. The XPS peak intensities were obtained after Shirley background removal and no relevant charging effect was observed. Freshly prepared samples were quickly (to avoid atmospheric doping) transferred into the XPS chamber. The base pressure of the chamber was maintained at approximately 5×10^{-10} mbar during the experiments.

A.4. Gas- sensing set-up

Functionalized epitaxial and quasi-freestanding graphene samples were measured in a gas flow Hall effect measurement system, as is schematically shown in figure A5, (Ecopia

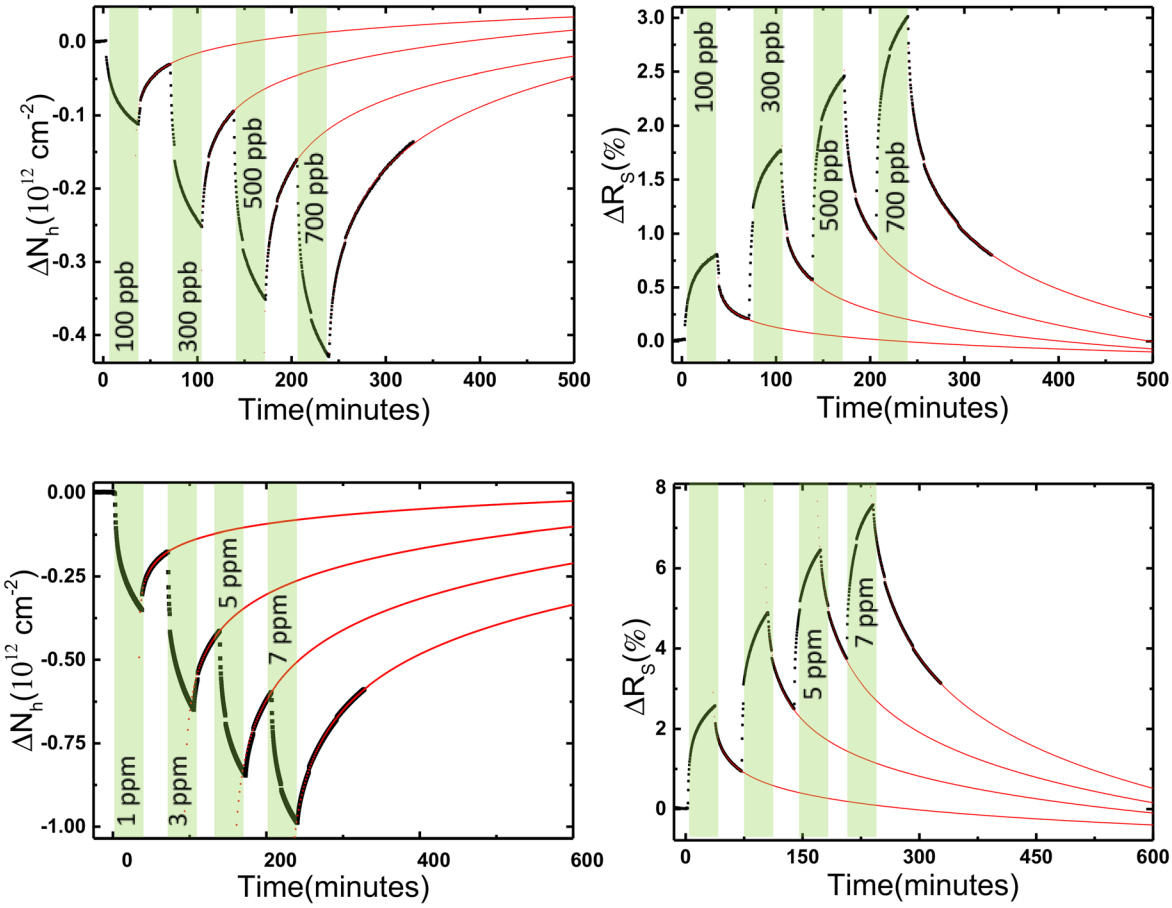

Figure A6. Carrier concentration (a) and relative resistance changes (b) of CoMP-QFeG sensor exposed first to pure N_2 and then to a sequence of 100 ppb ($t = 0$ min), 300 ppb ($t \sim 65$ min), 500 ppb ($t \sim 120$ min), 700 ppb ($t \sim 210$ min) of NH_3 gas. Carrier concentration (c) and relative resistance(normalized to the resistance value at $t = 0$ min) (d) changes of CoMP-QFeG sensor exposed first to pure N_2 and then to a sequence ($t = 0$ min) of 1 ppm, 3 ppm, 5 ppm, 7 ppm of NH_3 gas. Extrapolated recovery data (red curves in the graph) at figures shows that sensor can be completely recovered aproximately after overnight N_2 purge (All recovery curves tend to the same value after long N_2 exposure).

HMS-5500/AHT55T5, 0.546 Tesla), supplied with a constant 3 slm gas flow at atmospheric pressure and room temperature (25 C). Nitrogen (99.9995%, 5.5 N purity) was used as a carrier gas and NO_2 was supplied from a certified permeation tube (KIN-TEK) and diluted using a gas calibration system (MCZ CGM2000). NH_3 was supplied from a gas cylinder (Praixair 99.9995%, 5.5 N purity) connected to the gas calibration system. For the sensing experiments with humidity, the carrier gas was humidified by a controlled evaporation module (CEM, Bronkhorst) and added 1:1 to the diluted gas flow. With the CEM-system a defined amount of liquid provided by a pressurized water reservoir is vapourized and mixed with the carrier gas flow. The resistance and major carrier concentration of the device were measured using a four probe Van der Pauw configuration as is shown in figure 5. A constant current of 0.1 mA was applied to the sensor and the relative resistance change and major carrier concentration were recorded during gas exposure (signal to noise ratio at base line is $\Delta R/R = 10^{-4}$). Prior to the Hall measurements, the sample was annealed in the measurement system during 30 min at a temperature of 150 C under 3 slm pure N_2 flow.

A.5. DFT calculations for a Co porphyrin molecule adsorbed on graphene without taking the alkyl chains into account

We conducted spin polarized calculations within the LSDA taking into account electron correlations where an extra Hubbard-U term is introduced following the standard Duradev implementation for an on-site Coulomb interaction between localized orbitals, parameterized by $U_{\text{eff}} = U - J$, where U and J are the Coulomb and the exchange parameters as implemented in the SIESTA computational code [14]. A double-ζ basis set of localized atomic orbitals was used for the valence electrons. Sampling of the Brilouin zone takes place by a $(5 \times 5 \times 3)$ shifted Monkhorst–Pack grid [19], while a mesh cutoff energy of 200 Ry has been imposed for real-space integration. The structure has been relaxed until forces were less than 0.05 eV Å^{-1}.

A.6. Electronic calculations H_2O and porphyrin adsorption on quasi free standing graphene

The role of water in combination with porphyrin is investigated by an electronic structure calculation with both H_2O and

the Co-porphyrin molecule situated on graphene as shown in figure A3 of the appendix. The only difference is a 0.1 eV shift of the Co-3*d* state at 0.2 eV.

References

[1] Schedin F, Geim A K, Morozov S V, Hill E W, Blake P, Katsnelson M I and Novoselov K S 2007 *Nat. Mater.* **6** 652
[2] Dan Y, Lu Y, Kybert N J, Luo Z and Johnson A T C 2009 *Nano Lett.* **9** 1472
[3] Rumyantsev S, Liu G, Shur M S, Potyrailo R A and Balandin A A 2012 *Nano Lett.* **12** 2294
[4] Chen G, Paronyan T M and Harutyunyana A R 2012 *Appl. Phys. Lett.* **101** 053119
[5] Singh A K *et al* 2013 *Appl. Phys Lett.* **102** 043101
[6] Emtsev K V *et al* 2009 *Nat. Mater.* **8** 203
[7] Riedl C, Coletti C, Iwasaki T, Zakharov A A and Starke U 2009 *Phys. Rev. Lett.* **103** 246804
[8] Iezhokin I, Offermans P, Brongersma S H, Giesbers A J M and Flipse C F J 2013 *Appl. Phys. Lett.* **103** 053514
[9] Chaudhary A, Patra R and Rath S P 2010 *Eur. J. Inorg. Chem.* **33** 5211
[10] Auwärter W, Écija D, Klappenberger F and Barth J V 2015 *Nat. Chem.* **7** 105
[11] Liu S F, Petty A R, Sazama G T and Swager T M 2015 *Angew. Chem., Int. Ed.* **54** 6554
[12] Sugimoto H, Ueda N and Mori M 1981 *Bull. Chem. Soc. Japan* **54** 3425
[13] Cao Z, Chen Q, Lu Y, Liu H and Hu Y 2013 *Int. J. Quantum Chem.* **113** 1137
[14] Chilukuri B, Mazur U and Hipps K W 2014 *Phys. Chem. Chem. Phys.* **16** 14096
[15] Di Natale C, Buchholt K, Martinelli E, Paolesse R, Pomarico G and D'Amico A, Lundström I and Spetz A L 2009 *Sensors Actuators* B **135** 560
[16] Hoang M H, Choi D H and Lee S J 2012 *Synth. Met.* **162** 419
[17] Sun L, Gu C, Wen K, Chao X, Li T and Hu G 1992 *Thin Solid Films* **210** 486
[18] Liu Y, Liang Q, Chen F and Zhu D 1996 *Solid State Commun.* **99** 167
[19] Offermans P, Crego-Calama M, Brongersma S H 2012 *Sensors Actuators* **161** 1144
[20] Qiu X, Wang C, Zeng Q, Xu B, Yin S, Wang H, Xu S and Bai C 2000 *J. Am. Chem. Soc.* **122** 23
[21] Jarvinen P, Hamalainen S K, Banerjee K, Hakkinen P, Ijas M, Harju A and Liljeroth P 2013 *Nano Lett.* **13** 3199
[22] Altenburg S J, Lattelais M, Wang B, Bocquet M and Berndt R 2015 *J. Am. Chem. Soc.* **137** 9452
[23] Leenaerts O, Partoens B and Peeters F M 2008 *Phys. Rev.* B **77** 125416
[24] Wehling T O, Katsnelson M I, Lichtenstein A I 2009 *Chem. Phys. Lett.* **476** 125
[25] Benjamin A, Bhattarai F A, Mazur U and Hipps K W 2012 *J. Am. Chem. Soc.* **134** 14897
[26] Ristein J, Mammadov S and Seyller Th 2012 *Phys. Rev. Lett.* **108** 246104
[27] Lupo F, Tudisco C, Bertani F, Dalcanale E and Condorelli G 2014 *Beilstein J. Nanotechnol.* **5** 2222
[28] Alfredsson Y *et al* 2015 *Thin Solid Films* **493** 13
[29] Wackerlin C *et al* 2013 *Chem. Commun.* **49** 10736
[30] Scardamaglia M, Lisi S, Lizzit S, Baraldi A, Larciprete R, Mariani C and Bett M 2013 *J. Phys. Chem.* C **117** 3019
[31] Hermanns C F 2013 *PhD Thesis* Freie Universität, Berlin, p 50
[32] Bai Y *et al* 2009 *New J. Phys.* **11** 125004
[33] Castro Neto A H, Guinea F, Peres N M R, Novoselov K S and Geim A K 2009 *Rev. Mod. Phys.* **81** 109
[34] Soler J M, Artacho E, Gale J D, García A, Junquera J, Ordejón P and Sánchez-Portal D 2002 *J. Phys.: Condens. Matter* **14** 2745
[35] Monkhorst H J and Pack J D 1976 *Phys. Rev.* B **13** 5188
[36] Otsuki J 2010 *Coord. Chem. Rev.* **254** 2311–41
[37] Bagus P S, Staemmler V and Wöll C 2002 *Phys. Rev. Lett.* **89** 096104
[38] Zanjani S M M, Sadeghi M M, Holt M, Chowdhury S F, Tao L and Akinwande D 2016 Enhanced sensitivity of graphene ammonia gas sensors using molecular doping *Appl. Phys. Lett.* **108** 033106